The High Resolution Fly's Eye – Status and Preliminary Results on Cosmic Ray Composition Above 10^{18} eV

P. Sokolsky

High Energy Astrophysics Institute
University of Utah
Salt Lake City, Utah 84112, USA

ABSTRACT

We describe the current status of the High Resolution Fly's Eye detector. Event reconstruction and associated systematics for stereo reconstruction are discussed and recent preliminary results on the study of the composition of ultra-high energy cosmic rays by the Xmax method are presented. These results indicate that the composition of cosmic rays becomes predominantly light near 10^{19} eV and beyond.

Keywords: Cosmic rays, composition, atmospheric fluorescence, fly's eye, stereo detection

1. INTRODUCTION

The High Resolution Fly's Eye (HiRes) detector[20] is based on the pioneering Fly's Eye detector[1] which took data from 1981 to 1992. This was the first air fluorescence detector to produce significant physics results. The original detector demonstrated that monocular and stereo reconstruction of extensive air showers at distances of up to 20 km was possible. In addition, this detector produced monocular and stereo determinations of the cosmic ray spectrum[2], stereo determination of the cosmic ray composition[3], and a study of galactic anisotropy as a function of energy[4]. Papers setting limits on the cosmic neutrino flux[5] and determining the proton-air inelastic cross-section were also published[6]. The observation of an extraordinary event well beyond the Greisen-Zatsepin-Kuzmin cut-off with energy of 3 x 10^{20} eV generated a great deal of interest[7]. Apparent confirmation of events well beyond the GZK cutoff followed from the AGASA ground array experiment[8].

A proposal to build a much more sensitive atmospheric fluorescence detector was submitted to the National Science Foundation and the HiRes project was approved in 1994. This detector has an order of magnitude greater aperture than the original Fly's Eye as well as the present AGASA ground array(1000 km^2 str vs 100 km^2 str time averaged aperture) and significantly better energy and shower profile resolution. The stereo detector began to take data in 2000. Monocular data was taken with the first completed HiRes detector (HiRes I) since 1997 and results based on this data as well as the early monocular data from the HiRes II detector have recently been submitted for publication[9]. Here, we concentrate on preliminary results on cosmic ray composition from stereo data taken since 1999. The analysis forms the basis of a Ph.D. thesis by G. Archbold of the University of Utah.

The Fly's Eye experiment showed evidence that the cosmic ray spectrum was changing from a heavy to a light composition in the 10^{17} to 10^{18} eV region. This was confirmed by the HiRes prototype/MIA experiment[10]. However, very little statistics was available near and above 10^{19} eV. At the same time, various cosmic ray source models have been proposed which would result in either largely protonic, largely heavy (Fe) nucleus, or largely gamma ray enriched fluxes at the highest energies[11]. A determination of the cosmic ray compostion in this energy range is thus very important for discriminating between these models and elucidating the nature of the GZK cut-off region and beyond.

2. DETECTOR DESCRIPTION

The HiRes detectors consist of two sites (HiRes I and II) 12.6 km apart, located at Dugway Proving Ground in Utah, at an atmospheric depth of 860 g/cm^2. Each site consists of a large number (22 at HiRes I and 42 at HiRes II) of telescope units pointing at different parts of the sky. The detectors observe the full 360 degrees in azimuth but only cover from 3 to 16.5 (at HiRes I) and from 3 to 30 degrees (at HiRes II) in elevation angle. Since most cosmic ray events are detected

at distances of between 5 to 30 km from the detectors, the missing higher elevation angles contribute little to the event rate. Each telescope consists of a 3.72 m^2 effective area mirror and a 256 phototube camera cluster in the mirror's focal plane. The phototubes have flat hexagonal bialkaline photocathodes, each subtending a 1 degree by 1 degree field of view on the sky. They are arranged in a close-packed pattern with 16 columns and 16 rows. The tubes view signals thru a UV filter which cuts out light below 300 nm and above about 400 nm (corresponding to the strongest UV air-fluorescence range).
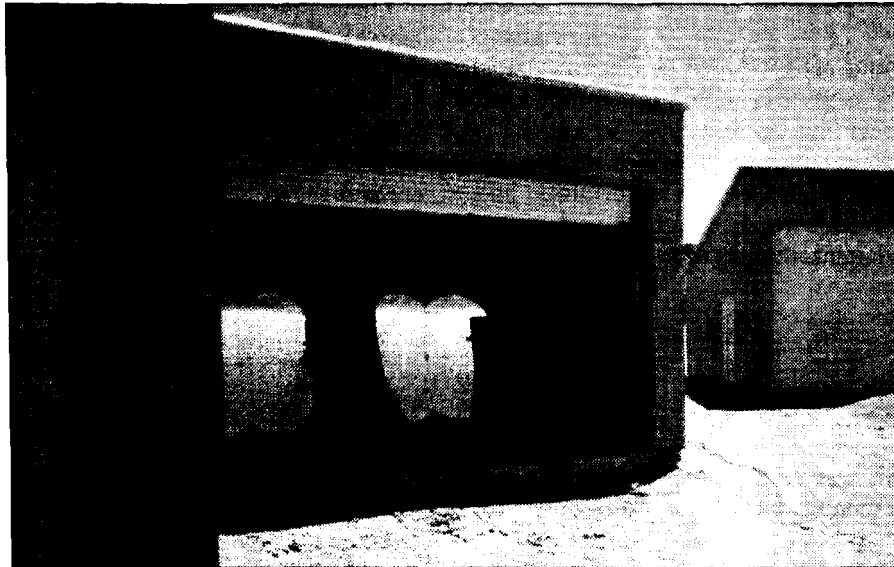

Figure 1: Detector Housing Showing Mirrors and Phototube Clusters.

The isotropically produced fluorescence light from a passing air shower triggers a succession of tubes. Each tube views the light produced at a particular depth in the shower development. If the shower geometry is known, measurement of the light intensity along the shower trajectory allows us to reconstruct the longitudinal shower development of the shower.

The HiRes 1 detector has a sample and hold electronics system which integrates the light signal in a 5 microsecond window if a tube signal exceeds a pre-set discriminator threshold. HiRes II has an FADC system which continuously digitizes the photmultiplier signals at 10 Mhz by 8-bit FADC's. At HiRes I, the singles rates for all tubes are held constant by adjusting the discriminator threshold as the sky noise changes. They can change on a minute to minute basis throughout the night. At HiRes II, more complex higher-level trigger decisions allow for lower effective thresholds with much slower adjustments. The triggering schemes for HiRes I and HiRes II are somewhat different, reflecting the differences in the electronics. At HiRes I, each 256 phototube cluster is divided into 16 subclusters. For an event in a cluster to be read out, we require two adjacent subclusters to trigger, where a subcluster trigger is defined as three tubes triggering within a pre-determined time window. Two of the three tubes must be adjacent to each other. At HiRes II sum signals from each row and column are generated and the lowest level trigger requires that several rows and several columns have a signal greater than a pre-set voltage within a gate time. For events meeting this requirement, a higher level trigger scans each tube to determine the presence of a signal and resulting triggered tubes are read out.

The arrival direction of the cosmic ray initiating the shower can be reconstructed monocularly, using the triggered photomultiplier pointing directions to determine the shower-detector plane, and the relative photomultiplier triggering times to determine the impact parameter and angle of the track within the plane. From this information, the impact parameter, zenith and azimuth angles can be easily calculated. This method relies on accurate measurement of signal arrival times and can be affected by how well the optical spot size on the cluster is understood, since variation in the spot size can affect time slewing. Stereo reconstruction affords much better precision. If the shower is detected by both HiRes I and II detectors and two shower-detector planes determined, the shower direction must lie along the intersection

of the two planes. Except for cases where the opening angle between the planes is very small, the stereo method produces much more exact reconstructions of event geometry. Because of the simplicity of the method, it is virtually impossible to get a systematically wrong shower direction and distance, once the pointing directions for the phototubes are accurately determined.

The HiRes detector can reconstruct showers as far away as 30-40 km. A typical shower is seen in 10-100 tubes and the tube signals last between .1 and 4 microseconds with a dynamic range of between a few to several thousand photoelectrons. The night sky noise varies slowly from 20 to 40 photoelectorns per microsecond per tube from dusk to dawn.

3. EVENT RECONSTRUCTION

Each HiRes detector triggers and operates independently of the other. Stereo events are formed by searching for coincidences between the two central GPS clock times latched by the event trigger. Most such stereo events are not cosmic rays but consist of artificial flashers and laser tracks used to characterize the atmosphere as described below. These sources are removed based on known geometry and timing information. Noise events are removed using a Rayleigh filter which demands that the probability that an event was created by random noise is less than 0.1 %. The axis of the cosmic-ray shower and the position of the HiRes detector uniquely define the shower-detector plane. An amplitude weighted fit is performed to the directions of the triggered tubes at each detector to determine the directions of the unit normal to each plane. This fit is iterated to remove residual noise tubes near the track.

The unit normal pointing accuracy is typically .5 degrees. Once the unit normals are determined, the intersection of the two planes gives the direction and location of the cosmic-ray shower axis. The plane fitting uncertainties are propagated to derive uncertainties in zenith, azimuth and impact parameter variables for the stereo event. Typical uncertainties in these parameters are 1 degree, 2 degrees and 100 meters respectively.

Once the geometry of the event is determined, the pmt signals can be used to determine the shower size (number of charged particles) in appropriate angular bins on the sky. In effect, the shower track is divided into one degree angular bins and the contribution of each tube signal to each bin determined. This contribution depends on the effective area of each pmt which is computed from a ray tracing table which accounts for cluster obscuration, gaps between pmts, spot size and spot position on the pmt. The resulting longitudinal shower profile still depends on knowledge of the air fluorescence efficiency and atmospheric attenuation – two major systematic issues for air fluorescence experiments. We will discuss these below.

Finally, combining the propagated bin signal and the geometry, the size of the shower as a function of atmospheric depth is determined, individually for each detector and combining data from both detectors for the best possible measurement. Forward beamed Cherenkov light scattered into the detector is subtracted in an iterative process.The individual measurements can be used to study detector resolution, since the same shower is measured independently twice, while the combined data is used for doing physics. The resultant shower profile is fit to a Gaisser-Hillas function which has been shown to be an accurate representation of shower development, both in Monte Carlo simulations and for real data[12]. The depth of shower maximum, Xmax, and shower energy are determined from this fit. The shower energy is proportional to the integral of the Gaisser-Hillas function after corrections are made for missing energy due to neutral particles or high-energy muons hitting the Earth's surface. The missing energy correction is typically no larger than 10%.

4. SYSTEMATIC ERRORS

There are many steps between event detection and determination of the shower energy and Xmax. In this paper we concentrate on the systematic issues that affect the determination of Xmax. These include precision of geometrical reconstruction and atmospheric corrections. Systematic effects due to uncertainties in our knowledge of atmospheric fluorescence efficiency, absolute detector calibration, and missing energy impact the determination of the cosmic ray spectrum, but are only second-order in determining the position of the shower maximum in the atmosphere and will not be discussed here.

1. Geometrical Reconstruction

The only significant systematic error in reconstructing the geometry of the events comes from uncertainties in the pointing direction of the mirrors and tubes. While theodolite methods have been used to set the mirror and tube directions initially, monitoring pointing accuracy over time using such techniques is tedious. Two related methods have been developed that are much simpler to implement. In the first case, a CCD camera is moved from mirror to mirror and mounted at the center of each mirror. The CCD camera is sensitive to faint stars. A comparison of known star positions to detected stars provides a very sensitive check of mirror alignment. The method has been used successfully and repeated at intervals. A second method is to use the phototubes themselves to look for stars[13]. The advantage of this method is that it provides a continuous geometry survey of all detector units on a nightly basis. However, since the pmt's view the sky through a UV filter, only UV emitting stars can be used. The basis of this method is the TD 1 Catalog of Stellar UV Fluxes. About 600 stars can be detected on an average night. As a star moves across the field of view of a pmt, the signal variance increases dramatically (since the pmt's are AC coupled to transmit fast pulses, slow light level changes are not directly measurable). A plot of signal variance as a function of time clearly depicts the passage of a bright UV emitting star. A peak finding algorithm has successfully found many such stars and correction parameters to the pointing directions of tubes generated. For most mirrors, correction parameters are small. No obvious tilt in any mirror/camera systems has been found relative to surveyed values, but some offsets corresponding to angular errors of 0.2 to 0.3 degrees have been discovered using this method.

2. Signal binning

Spherical mirrors produce optical spot sizes that suffer from spherical aberration. The pmt camera position has been optimized to minimize this effect, but it is still present to some degree. Furthermore, since the signal is contained in a spot which is typically spread across several tubes, the dead space between tubes and the spatial variation in photocathode quantum efficiency must be taken into account. All of this is done by careful ray-tracing from the light source at the shower, through the atmosphere to the mirror and to the phototubes. A good cross-check on the efficacy of this calculation is afforded by the star finding technique described above. A star image moving across the pmt cluster will map out all the optical aberration and dead spaces and the result can be compared to the ray tracing calculation. Fig 4 shows the effective spot size for a star at the center of a cluster and at the edge. The effect of spherical aberration is clearly shown. These spot sizes and their dependence on the distance from cluster center are in excellent agreement with ray tracing calculations, as is the estimate of dead space, which can lead to a decrease in signal of as much as 25% in the worst case.

3. Atmospheric Transmission

In the near – UV region the atmosphere is relatively transparent with very little absorption of light. Light extinction is mainly due to scattering, both from N_2 and O_2 molecules and from aerosol particles. The molecular component is well known and changes little from day to day. Molecular scattering is via the well-understood Rayleigh scattering mechanism. The aerosol component can change from night to night and from hour to hour. We determine the effect of aerosols by firing a UV laser whose energy is well determined from one of our detector sites and measuring the scattered light with the other detector site. The laser beam is steered through a variety of angles and probes most of the fiducial volume of interest. This data can be used to determine the aerosol scattering length, angular distribution of the aerosol scattering cross-section, scale height of the aerosol layer and other properties. Fig 5 shows an example of a particular near-horizontal laser shot. It shows the intensity of scattered light as a function of scattering angle. The data and the best fit to the data using a Monte Carlo combining the known molecular scattering and a four – parameter aerosol model are shown. The forward peak is characteristic of aerosol scattering, since pure Rayleigh scattering would generate a symmetric $1 + cos^2(\theta)$ distribution.

Such horizontal laser shots are used to determine the horizontal extinction length. A similar analysis of vertical shots is used to determine the vertical optical depth of the aerosols. The combined data is used to determine the aerosol scale height. Laser shots are fired in a fixed pattern on an hourly basis and atmospheric aerosol parameters are determined and tabulated with the same time sequence. Typical aerosol horizontal scattering lengths are 20-35 km and typical scale heights are .2 – 1.2 km. For comparison, the molecular horizontal scattering length at 355 nm is 18 km, while the molecular scale height is 7 km. Fig 6 shows the distribution of vertical OD and horizontal extinction lengths as well as the derived distribution of of aerosol scale heights over nearly two years of data.
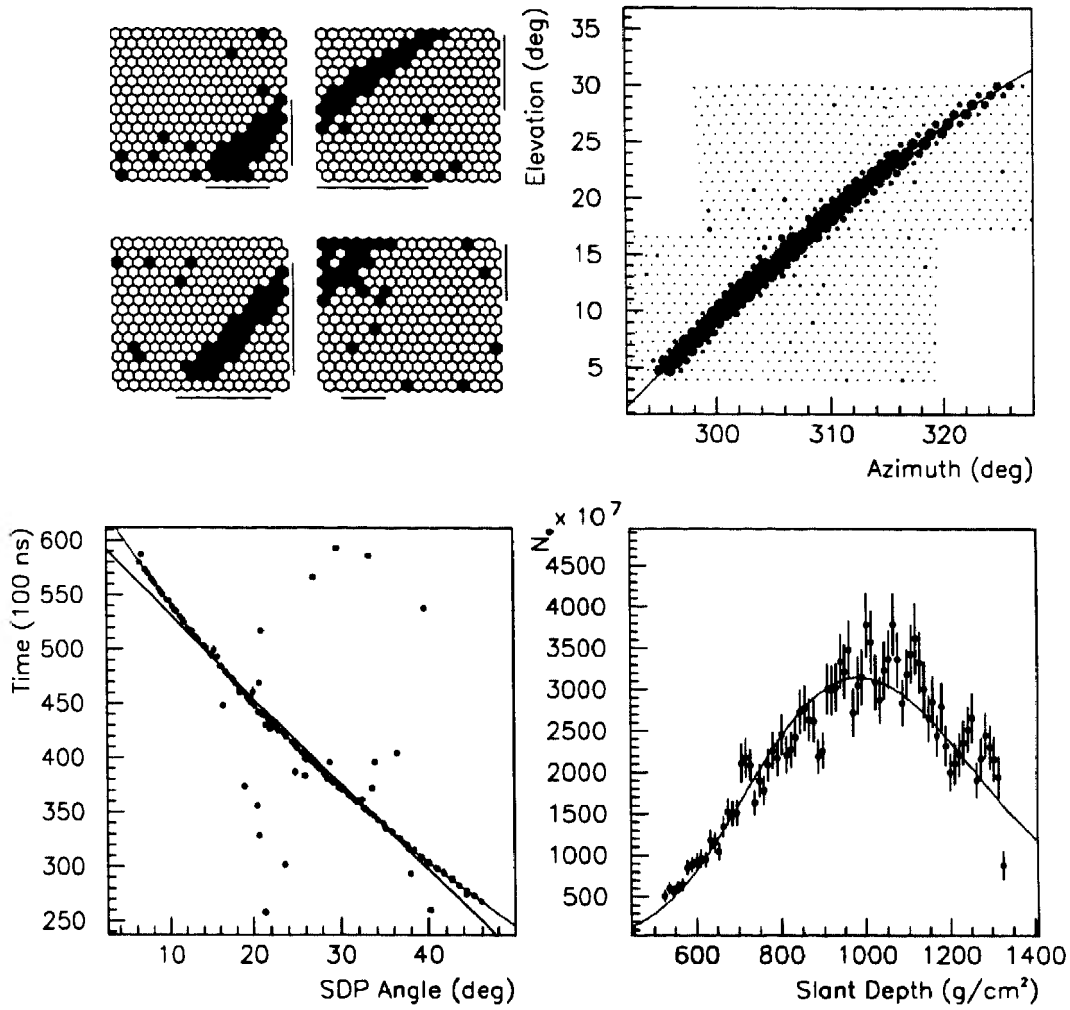
Fig. 3 Event Seen by Four Mirrors. Shower track propagating through mirrors (top); time vs. angle plot of signal arrival times (bottom left); reconstructed shower profile as function of depth (bottom right).
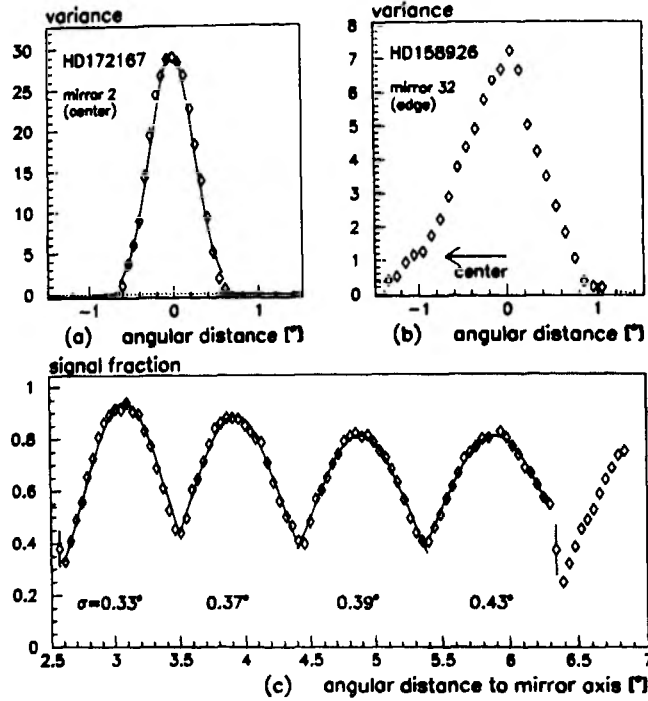
Fig. 4 Spot size as measured by star passage for a tube near the center of mirror (top left) and the edge of mirror (top right). Bottom shows effect of signal broadening as star passes away from mirror axis.

While the error on horizontal extinction are well-controlled, with a typical one-sigma variation of +/- 2 km on a mean of 24 km, the vertical OD has a systematic error of + .02 OD due to assumptions about the lack of aerosol scattering at altitudes above 3.5 km which are built into the analysis.
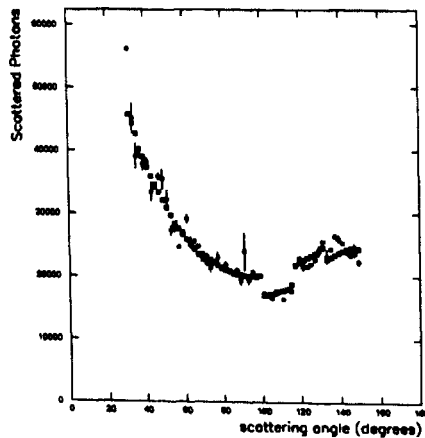

Fig. 5 Comparison of data(dark squares) and Monte Carlo (light squares) prediction for light scattered out of a horizontal laser beam.
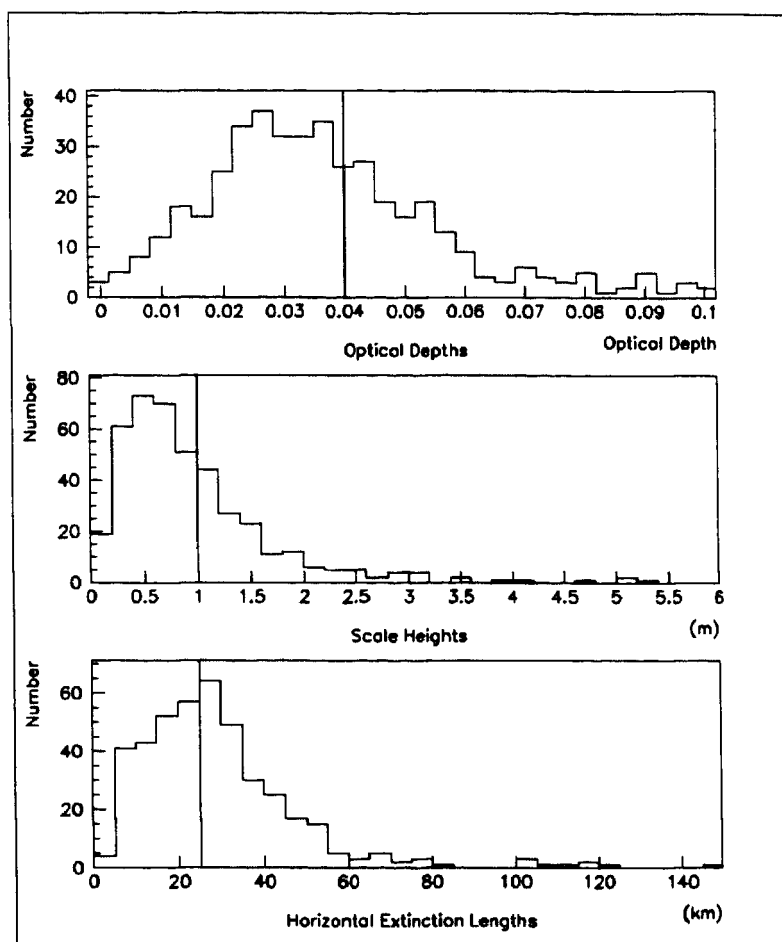
Fig. 6 Distribution of aerosol vertical optical depth (top), horizontal extinction length and derived scale heights from Several years of HiRes laser shots.

In addition to understanding atmospheric transmission, the laser data is used to test for the presence of clouds in the fiducial volume. Undetected clouds will reduce the effective aperture and could generate biases in the distribution of shower maximum positions (Xmax). An algorithm has been developed to exploit the obvious extra track width introduced by the presence of clouds. A pseudo-width is defined as the product of off-track distance of triggered tube and the tube signal divided by the laser energy. The total pseudo-width, divided by track length is found to be a sensitive measure of the presence of clouds. This information is used in conjunction with IR cameras that detect the presence of clouds by temperature differences.

5. THE XMAX METHOD FOR DETERMINING COSMIC RAY COMPOSITION

The distribution of positions of shower maxima (Xmax) in the atmosphere has been shown to be sensitive to the composition of cosmic rays. It is well known that for any particular species of nucleus, the position of shower maximum will deepen with increasing energy as the logarithm of the energy. This is known as the elongation rate. Heavy nuclei are expected to have larger inelastic cross-sections and hence the shower resulting from the first interaction will begin at shallower atmospheric depths. In addition, heavy nuclei of atomic number A can be thought of to be superpositions of A nucleons. The resultant shower is then, crudely, a superposition of A subshowers each with E/A of the initial energy. Such a shower will have reduced fluctuations and a shallower depth of maximum position than a proton or a light nucleus of the same energy. While the details are dependent on the hadronic model assumed, all modern hadronic

models give approximately the same elongation rate (between 50 and 60 gm/cm^2 per decade of energy) and agree within about 25 gm/cm^2 on the absolute position of the average shower Xmax at a given energy for a given species. The sensitivity of an Xmax measurement to composition comes from the fact that the mean Xmax for Fe and p is about 75 – 100 gm/cm^2 different, independent of model. Fig 9 shows two current model predictions (QGS-Jet and SIBYLL) for the elongation rate for an Fe and p cosmic ray flux. A change in the composition from heavy to light in any particular energy decade would result in a much larger elongation rate than the 50-60 gm/cm^2 per decade number expected for a constant composition, while a change from light to heavy would lead to a negative elongation rate. Differences due to hadronic models for the same composition are much smaller.

Previous experiments[3,10] (Stereo Fly's Eye, HiRes/CASA/MIA hybrid experiment) have shown evidence for an elongation rate of 80 to 90 gm/cm^2 in the energy range from 10^{17} to $10^{18.5}$ eV. No information has been hitherto available on the behavior of the elongation rate near 10^{19} eV and above. The present HiRes stereo experiment is the first to have significant statistics and sufficient control of systematics to reach the 10^{19} eV and above region of interest.

4. Monte Carlo Simulations

Because the method entails comparing theoretical predictions of Xmax distributions as a function of energy with real data and using the comparison to learn about the composition of cosmic rays, all detector biases and resolutions must be adequately modeled in the simulation of the predictions. A detailed Monte Carlo simulation of HiRes I and HiRes II has been developed and carefully tested. The input to the Monte Carlo is either a set of monoenergetic simulated showers (generated by the program CORSIKA using the QGS-Jet or SIBYLL model for proton and Fe primaries) or a set of similar showers whose energy is chosen according to a power law spectrum. The showers are thrown at various impact parameters and angles until their simulated signals trigger the detector. Once triggered, a fake data file is written which can be analyzed by the same reconstruction programs used for data.
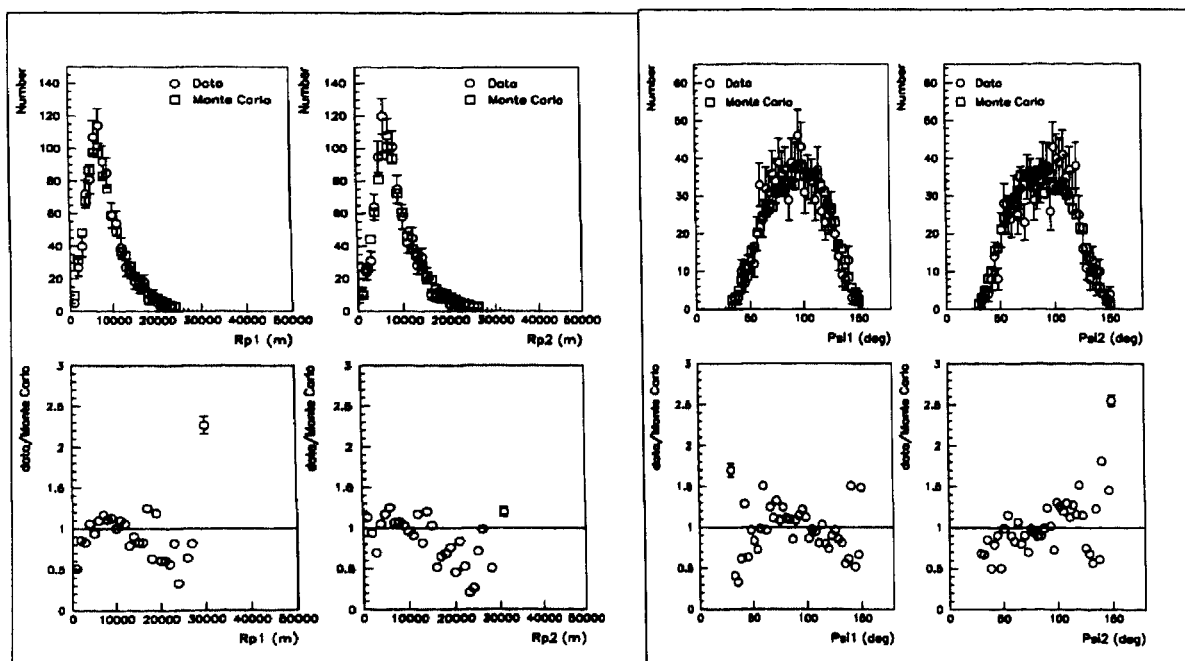

Fig. 7 Data and Monte Carlo Prediction of Rp (left) and Psi angle (track angle in the shower-detector plane) (right). Bottom shows ratio of data to MC.

While it is straightforward to check the detector resolution in energy and Xmax (or any other measurable variable) by comparing MC input values to reconstructed values, this is only meaningful if the Monte Carlo adequately simulates the operation of the detector. To check this we compare distributions in various measured variables. As an example, Fig 7

shows the measured and predicted Rp, and psi angle (the track angle in the shower-detector plane) distribution assuming a power law input spectrum consistent with the previously measured Fly's Eye stereo spectrum. Good agreement for this and other variables is observed. An additional important cross-check on the predicted Xmax resolution can be obtained by comparing the pull distribution ((Xmax I − Xmax II) / ((XmaxI + XmaxII)/2) for data and MC. This can only be done for a subset of the data, since not all events have the shower Xmax seen by both HiRes I and II. Fig 8 shows the result. There is excellent agreement between the MC predic tion (a Gaussian fit sigma of .09) and the data (a sigma of .10) for this subset. We can conclude that the detector resolution is well modeled by the Monte Carlo. After final cuts described below, the Monte Carlo predicts a resolution in Xmax of 37 gm/cm^2 and a 13% resolution in event energy.

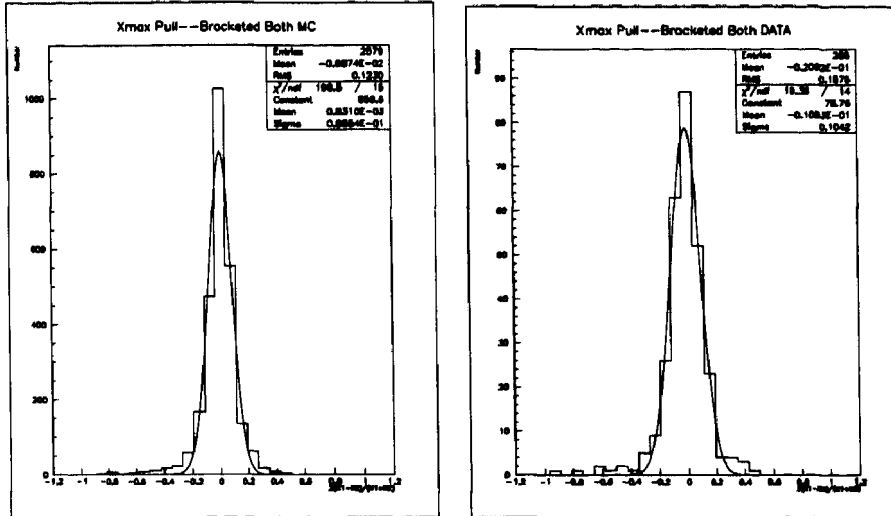Fig. 8 Pull distribution (Xmax I − Xmax II/ (Xmax I + Xmax II)/2) for data and Monte Carlo. Function represents a Gaussian fit to the data. The Gaussian fit has sigma of .1 for data and .09 for the Monte Carlo simulated events.

5. The Elongation Rate and Xmax Distributions

The present data set consists of events collected in stereo from Nov, 1999 to September 2001. A total of 1198 stereo events were found. After a minimum set of cuts to remove noise and events which can not be well reconstructed, and a requirement that either hourly atmospheric parameters exist for the time of the event with a VOD less than .12 or that excellent cloudless weather prevailed during that night, we are left with a total of 842 events, with energies ranging from $10^{17.7}$ to 8 x 10^{19} eV. Additional cuts which require that the shower maximum be directly visible in at least one of the detectors further reduces the data set to 723 events. Hourly atmospheric characterization (horizontal extinction length and scale height) was available for about ¾ of this data set. For the remaining ¼ of the data we use the average atmospheric parameters. There are no significant differences in any distributions of interest between these two data subsets.

Fig 9 shows the mean Xmax vs energy for data and for pure proton and Fe showers generated by either QGS-JET or SIBBYL after passing through the detector Monte Carlo. Shown on the same figure is data from the hybrid HiRes Prototype/MIA experiment which was sensitive to a lower energy range. The two experiments agree well in the region of overlap. The elongation rate plot indicates good agreement with the hypothesis that the composition of cosmic rays changes from heavy to light between 10^{17} and 10^{18} eV and remains constant above that energy. Fig 10 shows the width of the Xmax distribution in three energy bins. Also shown are prediction for a pure Fe composition. It is clear that the

data is incompatible with a heavy composition. It is in better agreement with pure protons. A two component (Fe and proton) fit to the measured Xmax distribution leads to between 55 and 80% protons for the SIBYLL and QGSJET models respectively.

6. Discussion

Detailed comparison between data and MC simulated events is possible because the intrinsic resolution function in Xmax is well understood in this experiment. However, it is possible that the atmospheric extinction is underestimated. We study this effect by changing the hourly atmospheric parameters available for each event by the maximum systematic shift (.02 VOD) and re-reconstructing the events. The effect on the elongation rate and the shower width distribution is small. The determination of Xmax is very insensitive to atmospheric parameters and while the energy of the event does shift (by about 10%) the logarithmic energy dependence makes the impact of this shift irrelevant for the elongation rate. MC studies show no significant differences in input and reconstructed elongation rate, indicating that the detector acceptance is not biasing the measured elongation rate. We also study the systematic uncertainty on the absolute value of the average Xmax by varying the mirror pointing directions, column depth of the molecular atmosphere as determined by balloon soundings and Cherenkov light subtraction algorithm, within one sigma systematic bounds. The resultant systematic shifts in Xmax near 10^{19} eV are 15,10, and 1 gm/cm^2 respectively. Taken in quadrature, the systematic error on absolute Xmax position is ~ 20 gm/cm^2.
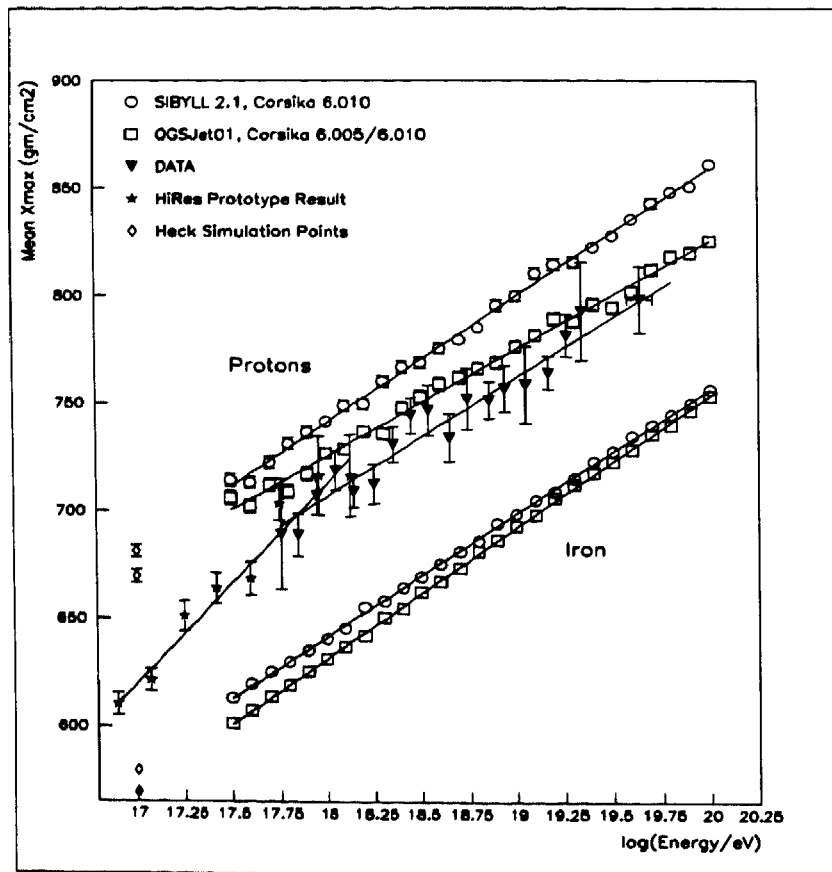

Fig. 9. Elongation Rate of HiRes stereo data set (triangles) and HiRes prototype/MIA data (stars). Open symbols show expected elongation rate for pure proton or pure Fe flux for two models of the hadronic interactions as implemented in CORSIKA.

Taking these systematic errors into account, it is very difficult for the elongation rate or the absolute position of Xmax to change significantly. It is thus not possible to accommodate significant heavy nucleus contribution to the cosmic ray flux above 10^{18} eV given the hadronic models presently at hand. We note that a light, largely protonic composition together with the HiRes monocular spectrum result, is quite consistent with a universal distribution of cosmic ray sources as originally envisaged by the GZK authors[16], or with a modified GZK scenario where the source distribution follows the large scale structure of galaxies[17]. The present data does not, however, have significant statistics near 10^{20} eV, and dominance of this flux by gamma rays, or a return to a heavy composition, as has been suggested by a number of authors[18], is still possible in this region. Elucidation of the composition in this region awaits further statistics from HiRes and new data from the Pierre Auger experiment[19].
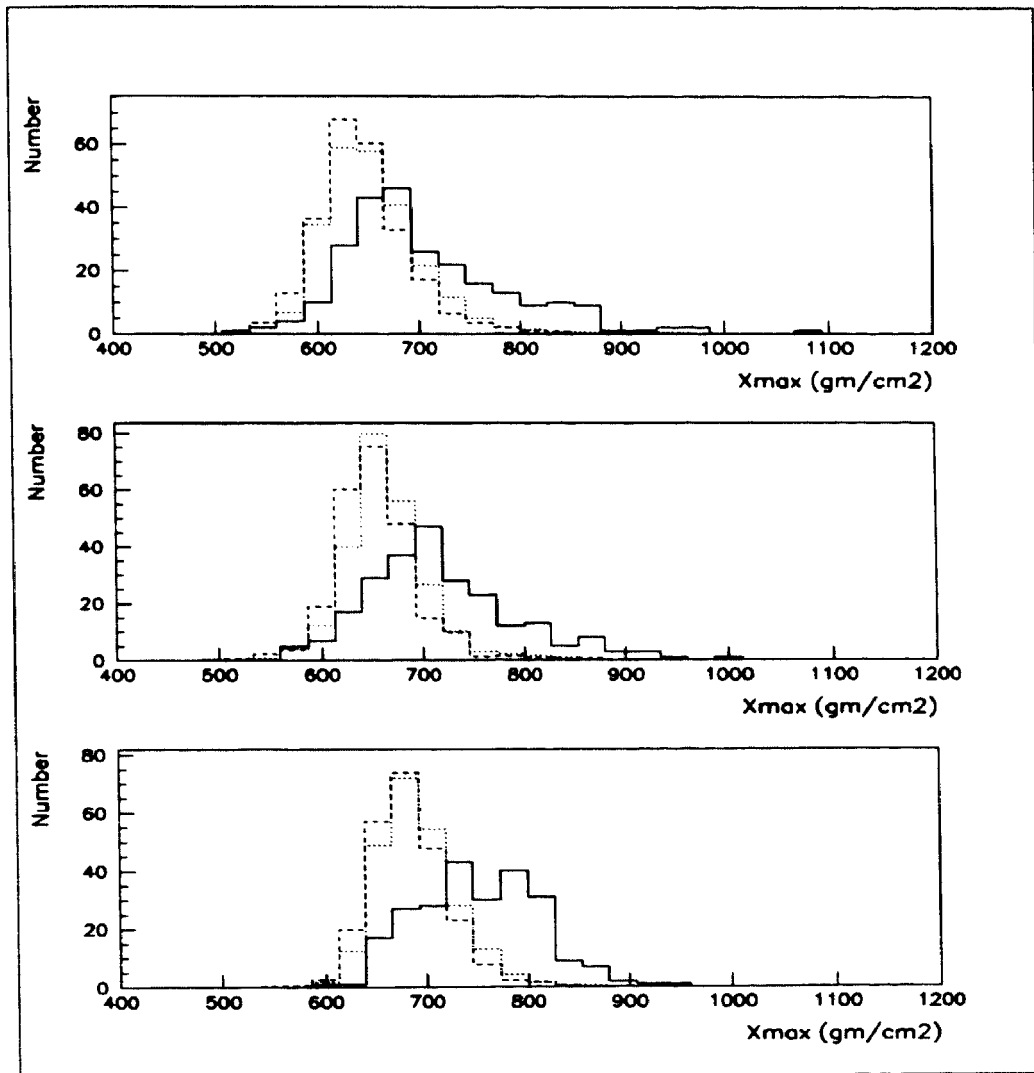

Figure 10. Xmax distribution of data in three energy bins (logE < 18.1 – top; 18.1<logE<18.4- middle; logE>18.4-bottom. Also shown is the prediction for pure Fe flux based on QGJ-jet (dashed lines) and SIBYLL(dotted lines) hadronic models for a pure Fe flux..

6. REFERENCES

1. R.M. Baltrusaitis et al.,"The Utah Fly's Eye Detector", *Nuclear Instruments and Methods, A240*, pp. 410-428, 1985.
2. D.J. Bird et al.," The Cosmic Ray Spectrum Observed by the Fly's Eye", *Astrophysical Journal 242*, p. 491, 1994.
3. G. Cassiday et al., *Astrophysical Journal, 356*, p. 669, 1990.
4. D. J. Bird et al., "Study of Broad-scale Anisotropy of Cosmic-Ray Arrival Directions From 2×10^{17} to 10^{20} Electron Volts From Fly's Eye Data", *Astrophysical Journal, 511*, pp. 739-749, 1999.
5. R. M. Baltrusaitis et al.," Limits on Deeply Penertrating Particles in the UHE Cosmic Ray Spectrum", *Phys. Rev. D, 31*, p.2192, 1985.
6. R. M. Baltrusaitis et al., "The Proton-Air Inelastic Cross-section measured by the Fly's Eye", *Phys. Rev. Lett., 52*, p. 1380, 1984.
7. D. J. Bird et al., "Detection of a Cosmic Ray with Measured Energy Well Beyond the Expected Spectral Cutoff due to Microwave Radiation", *Astrophysical Journal, 441*, 1995.
8. N. Sasaki, *Proc. Of the 27th Int. Cosmic Ray Conf. (Hamburg), 1*, p. 333, 2001.
9. T. Abu-Zayyad et al., *Phys. Rev. Lett.*, submitted 2002.
10. D. J. Bird et al., "Evidence for Changing of Cosmic Ray Composition between 10^{17} and 10^{18} eV from Multicomponent Measurements", *Phys. Rev. Lett., 84*, p. 4276, 2000.
11. See for example, P. Bhattcharjee and G. Sigl, *Physics Reports, 327*, p 109, 2000.
12. T. Abu-Zayyad et al., " Study of Longitudinal Development of EHE Cosmic Rays", *Astroparticle Physics, 16*, p.1, 2001.
13. P. A. Sadowski et al., "Geometry and Optics Calibration for Air Fluorescence Detectors Using Starlight", *Astroparticle Physics*, accepted for publication, 2002.
14. T. Abu-Zayyad et al., "Determination of Atmospheric Extinction and Scattering Using the HiRes Detector and Steerable Laser Beams" *Astroparticle Physics*, in preparation.
15. D. Heck et al.,"CORSIKA: A Monte Carlo Code to Simulate Extensive Air Showers", *Report FZKA 6019, Forschungszentrum Karlsruhe*, 1998.
16. K. Greisen, *Phys. Rev. Lett., 16*, p. 748, 1968; G. T. Zatsepin and V. A. K'uzmin, *Pis'ma Zh. Eksp. Teor. Fiz. 4*, p. 114, 1966 [*JETP Lett., 4*, p. 78, 1966.
17. A. V. Olinto, *Physics Reports, 333-334*, p. 329, 2000.
18. G. Sigl, D.N. Schramm, and P. Bhattacharjee, *Astroparticle Physics, 2*, p 401.,1994.
19. M. Boratov, "The Pierre Auger Observatory Project: An Overview" *Proc. Of 25th International Cosmic Ray Conference, Durban, Vol. 5*, p. 205, 1997.
20. The HiRes Collaboration consists of: B. Dawson, R. Clay (Univ. of Adelaide), J. Boyer, B. Knapp, E. Mannel, M. Seman, S. Westerhoff (Columbia University, Nevis Labs), W. Lee (Columbia University), J. Belz (Univ. of Montana), J.A.J. Matthews, M. Roberts (Univ. of New Mexico), D. R. Bergman, L. Perera, S.R. Schnetzer, G.B. Thomson (Rutgers University), M. Sasaki (University of Tokyo), T. Abu-Zayyad, Z. Cao, P. Huentemeyer, C.C.H. Jui, D.B. Kieda, E.C. Loh, K. Martens, J.N. Matthews, P. Sokolsky, R. W. Springer, L.R. Wiencke (University of Utah).